

Soft Sensorized Physical Twin for Harvesting Raspberries

Kai Junge & Josie Hughes

Abstract—The use of robotic systems for harvesting of crops is a growing application domain in the agriculture sector. A key challenge is to develop robotic systems to harvest soft fruits such as raspberries which require delicate handling as they are easily damaged. Designing and optimizing a robotic harvesting setup by testing on real raspberry crops can be challenging due to the short natural harvesting period and the cost and logistical challenges of running experiments in the field. To solve this problem, we present a sensorized physical twin of a raspberry which can be used to develop robotic harvesting systems before deploying in the field. The sensorized raspberry has the capability of measuring the applied forces before and after it has been picked off the plant with a high sensitivity. The mechanical design was optimized and a material with properties similar to the real fruit was chosen, in order to achieve similar mechanical properties to a real raspberry, specifically the stiffness before and after picking and the pulling force. The paper concludes with a harvesting demonstration performed by a robotic gripper, where the sensorized raspberry is used to assess the quality of the picking action. This work aims to lay the groundwork for accelerating the future development of robotic harvesting systems to enable robust development in a lab before deployment in the field.

I. INTRODUCTION

Robotics has an increasing role to play in agriculture to enable the food demands of the ever-growing population to be met [1]. One key area where robotics can contribute is harvesting. Due to social-economic pressures and the challenging nature of the work, there is a shortage of workers in recent years, resulting in up to 40% of yields remaining unpicked [2]. This waste has significant environmental and financial costs. One specific area still requiring much manual work is the harvesting of soft fruit, of which one of the most challenging is raspberries [3]. Although there has been a wide number of attempts to develop robotic solutions to harvest raspberries [4], [5] and other soft fruit [6], [7], their development is limited by the challenges associated with testing and developing robotic solutions [8].

The interactions between a robot gripper and the soft fruit are highly complex and thus challenging to simulate or model, requiring real world experiments. However, these require physical “field tests” out of the lab which limits the speed of iteration and development. This is further constrained by the limitation that raspberries are only ripe and ready for harvest for a few months out of the year. Furthermore, quantitatively evaluating the harvest quality is challenging, which is necessary for certain data driven methods to improve the hardware and/or the control policy. In summary, we need to develop experimental techniques to

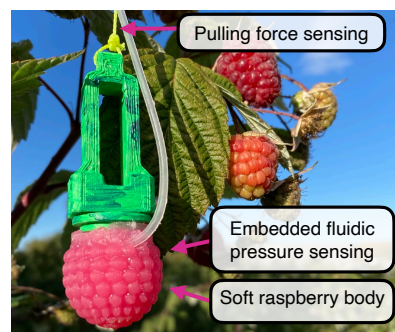


Fig. 1: Summary of the main characteristics of the sensorized raspberry.

overcome such practical limitations associated with developing harvesting robotics.

One approach to tackle this problem is to simulate the physical interactions through the development of “physical twins” - an artificial system which aims to imitate or replicate a physical system. The concept of physical twins have been explored in the past to aid the development of processes or interactions which are challenging to simulate or visualize [9]. Widely explored for applications in medicine, these physical twins or “phantoms” aim to artificially imitate a real world interaction to enable robots to learn how to perform medical tasks or processes [10]–[12]. In addition, they can be sensorized to provide feedback to aid the design of the robotic system. These approaches have been shown to have a significant impact in enabling increasingly rapid testing and development of medical robotics. Similar concepts have also been used in arable agriculture, most notably in the development of physical simulators of bovine milking udders for testing of automatic milking systems [13].

To address the challenges of undergoing harvesting research we apply soft-robotic techniques and methods to create a sensorized physical twin of a raspberry. By developing a novel design and accompanying fabrication pipeline, we aim to show how the reality gap between our soft sensorized raspberry and the real fruit can be closed. In particular, we focused on the picking force and the stiffness profile on and off the plant. By varying design parameters we also show that the parameters can be altered to simulate variation with the crop. By introducing fluidic sensing [11] into this small form factor we can record the forces exerted onto the simulated fruit which can be used to evaluate the performance of robotic picking experiments. Whilst we focus on raspberries, the approach could be extended to other crops.

For a sensorized twin which mimics the real fruit’s mechanical properties, we demonstrate how the physical twin can be used. Firstly, we show how the sensor how the sensor response can be used to identify key events during

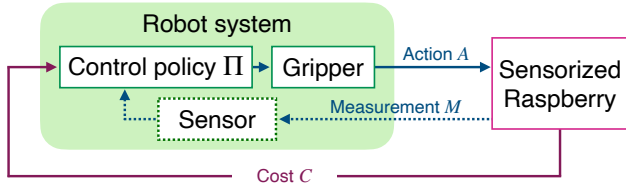


Fig. 2: Control/optimization loop illustrating how the sensorized raspberry can be used to improve real raspberry harvesting.

the picking process. Likewise, with a simple torque controller on a robotic gripper we show how the sensorized raspberry can be used to provide feedback or evaluate the quality of picking and to optimize a controller. This demonstration also highlights how such a simple controller is insufficient to harvest raspberries, and a more intelligent approach which leverages sensory-motor co-ordination is required.

In the remainder of this paper we first present the methods developed for the fabrication and sensorization of the raspberry. The experimental setup developed to evaluate the raspberry and the corresponding results are then provided, before which we conclude with a discussion.

II. METHODS

A. Problem Statement

1) *Assisting robotic harvesting*: Fig. 2 proposes the high level control/optimization concept of how this sensorized physical twin of a raspberry can be used for optimizing the robotic harvesting process. A robot system equipped with a gripper and sensors (e.g.: tactile sensors, force/torque sensors) can harvest the sensorized raspberry via some picking action A . This action could be preformed through a control policy Π using the robot’s sensor measurements M . Throughout the picking process, the quality of the picking motion can be evaluated by a cost C (calculated through the sensors on the physical twin) - which then can be used to improve upon Π or even the hardware design.

In this paper, we demonstrate a proof of concept of this optimization loop through a simple control policy Π and cost metric C . The dotted lines on Fig. 2 represents the future work which has not yet been implemented.

2) *Physical characteristics of raspberry harvesting*: To develop a physical twin which behaves as closely as a real raspberry, we identified key physical characteristics that must be matched. Considering the physical structure, a raspberry can be thought to be comprised of two components: the fruit and the receptacle. The receptacle is the “inner” part where the red fruit connects to the plant. When harvesting a raspberry, we can assume there are two dominant forces: F_p the force required to pull the raspberry, and F_c the force compressing the raspberry shown in Fig. 3a. A critical observation from real raspberries is the compression stiffness reduces significantly when the fruit is picked from the receptacle, i.e.: $k_{on} > k_{off}$ as shown in Fig. 3b and c.

Other relevant characteristics include the surface properties such as the geometry of the “dimples” and the friction coefficient. While the “dimples” were incorporated in the design, the friction has not been considered.

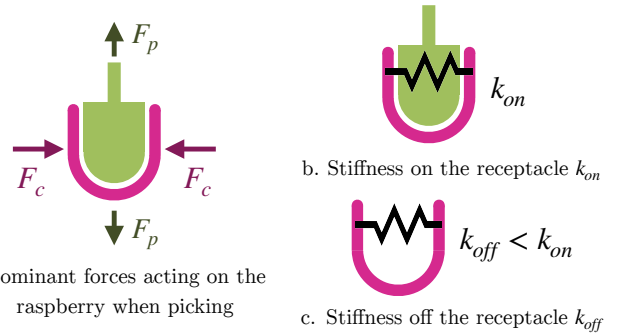


Fig. 3: Diagrams to show the key characteristics for harvesting raspberries: the pulling and compression forces, and the stiffness of the raspberry on and off the receptacle.

B. Raspberry design and fabrication

The goal for this physical twin is to design and fabricate a soft sensorized fruit which can be placed on a rigid receptacle. The sensorized fruit should be able to measure the compression force F_c both on and off the receptacle. While on the receptacle, the pulling force should also be detected. Finally, the design should allow for the maximum F_p and k_{on}, k_{off} to be variable to match that of a real raspberry.

The proposed design uses Dragon Skin™ 10 Fast[14] silicone for the soft “fruit” and 3D printed PLA for the rigid “receptacle”. The compression force F_c is measured through a fluidic sensor which monitors the pressure changes induced by the deformation of the fruit [11], [15]. This is achieved through a soft silicone tube (2mm ID x 4mm OD) embedded and sealed inside the fruit which connects to the fluidic sensor. When the tube deforms the volumetric changes causes a change in pressure within the tube. The pulling force is generated by a Neodymium magnet embedded in both the fruit and receptacle, where the separation can be tuned to vary the maximum pulling force (the force between two magnetic poles varies with $1/r^2$). The pulling force is measured by a load cell connected to the receptacle by a string. The stiffness profiles of k_{on} and k_{off} will be varied by changing the thickness of the silicone layer of the fruit.

To understand how best to match physical characteristics of a raspberry, two design types (A and b) were considered. Fig. 4 shows the internal structure of the two designs.

Both design types incorporates the necessary functionality discussed, but differ in the structure and fabrication pipeline. In type A, the tubing rests on an inner layer of silicone, which is then coated by a secondary outer layer. In type B, the tubing is directly embedded in the single silicone layer. In the fabrication process shown in Fig. 5, 3D printed inverse moulds are used to cast the silicone into the shape of the fruit. While type A has more parts and two moulding stages, it is overall simpler to fabricate than type B - requiring less “skillful” fabrication procedures. However, type B with the single silicone layer can achieve a lower k_{off} when compared to type A, which is a desired property.

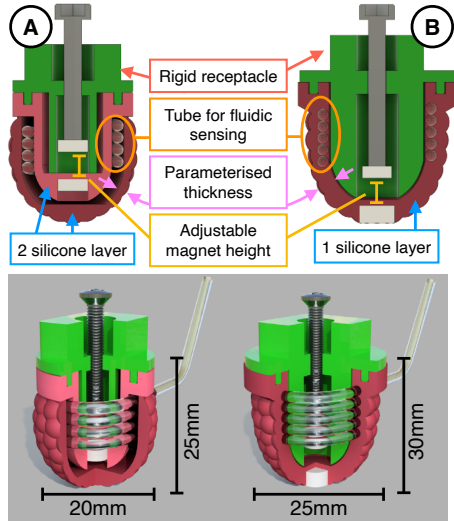
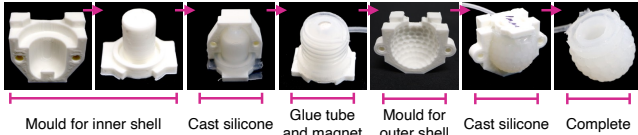


Fig. 4: Two proposed designs to fabricate the sensorized raspberry: Type A and B. Top: Cross section sketch with relevant characteristics and tunable parameters. Bottom: 3D render of the two designs showing the internal structure, outer surface, and its dimensions.

Raspberry type A



Raspberry type B

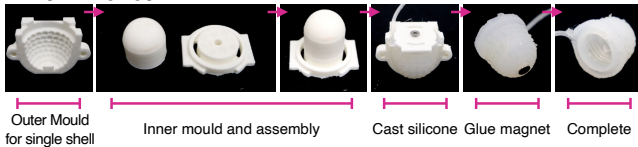


Fig. 5: Fabrication process for the two raspberry design types A and B.

III. EXPERIMENTAL SETUP

A. Main measurement setup

To be able to close the reality gap the variation of F_c with compression distance d and the pulling force F_p a mechatronic setup (see Fig. 6) has been created. The setup includes a 3kg load cell connected to a high resolution amplifier (HX711) used to retrieve the ground truth force readings. To measure F_c vs d , a stepper motor connected to a lead screw will linearly actuate a 3D printed part to compresses the raspberry against the load cell. From the other end of the load cell, a string which can be connected to both real and sensorized raspberries measures F_p . Sensor measurement readings and stepper motor control signals are all regulated by a Arduino microcontrollers.

B. Sensing inside the physical twin

To measure the compression of the raspberry (both on and off the receptacle), a high precision analog pressure transducer (MPXH6115A) is connected to the silicone tube embedded inside the raspberry utilizing “fluidic sensing” [15], [16]. The fluidic pressure transducer provides an analog signal that is proportional to that of the input pressure. In this experiment, the analog to digital converter (ADC)

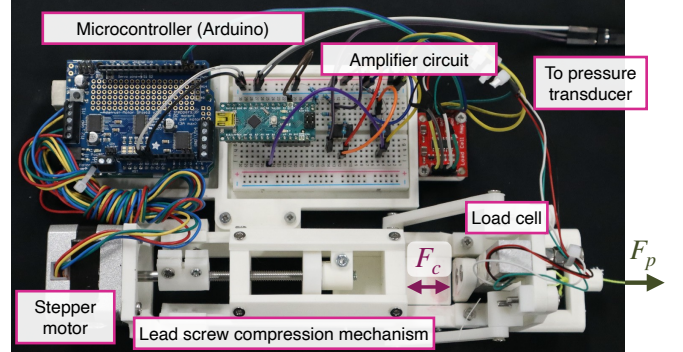


Fig. 6: Custom experimental setup for testing the measuring the stiffness and pulling force of real and sensorized raspberries.

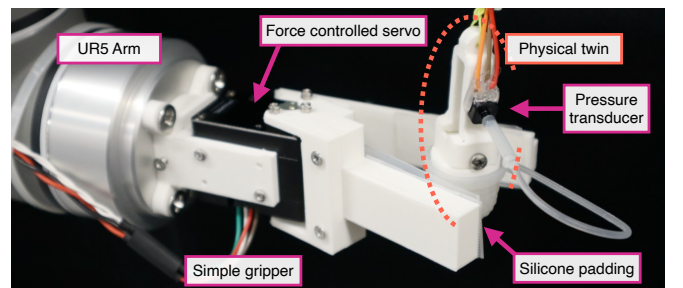


Fig. 7: Robot arm and gripper setup to pick the sensorized raspberry.

of the Arduino Nano (10 bit quantization, 5V reference voltage) is used. Since the pressure change due to deformed raspberry is minimal, the ADC quantization is not sufficient. Therefore, the raw signal is amplified after removing a voltage offset through an operational amplifier circuit, to ensure the amplitude of the analog signal is not limited by the quantization voltage. For this experiment, the voltage into the ADC has been amplified to be in the order of 100mV. The pulling force is measured by the same load cell mounted on the measurement setup shown in Fig. 6.

C. Robot harvesting demonstration

To demonstrate the control/optimization process discussed in Fig. 2, a simple gripper was developed as shown in Fig. 7. The gripper has two 3D printed “fingers” made from PLA and uses a Dynamixel servo (XM430-W210-R) to actuate one of the two fingers. A thin layer of Dragon Skin™ 10 is attached to increase gripping friction. The gripper is attached to a Universal Robots™ UR5 robot arm.

For this demonstration, the simplest control policy Π is considered, which is to close the gripper by applying a constant torque by the servo motor on the actuated finger (via constant current control). The picking action A is a linear motion of the arm moving directly downwards while closing the gripper. The motor current set-point (and thus the gripper torque) is the adjustable parameter, where an optimal value can be determined by assessing a cost metric.

IV. RESULTS

In this section we first present results highlighting how the physical properties of the sensorized raspberry can be tuned to close the reality gap. Secondly, we characterize the sensing properties of the raspberry with the embedded fluidic sensor.

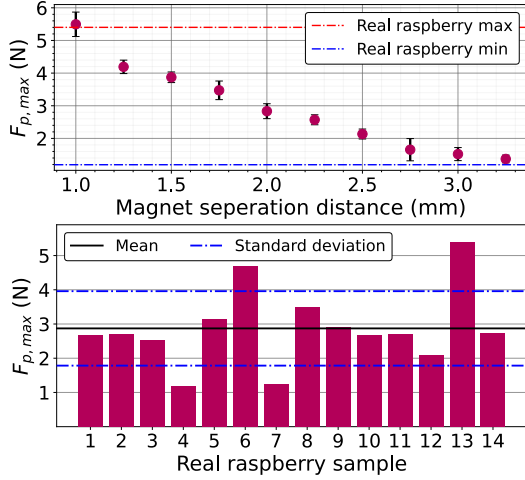


Fig. 8: Top: $F_{p,max}$ of real raspberries. Bottom: $F_{p,max}$ of the sensorized raspberry plotted against magnet separation distance.

We finally conclude with two harvesting demonstrations using the sensorized raspberry. Throughout this section, we will focus on a single raspberry design (a variant of Type B) which best closed the reality gap.

A. Closing the Reality Gap

1) *Maximum pulling force $F_{p,max}$* : To characterize the range of $F_{p,max}$ on real raspberries, a representative sample of 14 fresh raspberries were tested using the measurement setup discussed in III-A. From Fig. 8 we see how most raspberries require just below $3N$ to be harvested, while the overall range varies between $1.2 \sim 5.4N$. Thus, the ability to tune $F_{p,max}$ in this measured boundary is important.

To demonstrate the tuneability of the sensorized raspberry, Fig. 8 shows $F_{p,max}$ for different separation between the two magnets within the physical twin. The plot shows how the separation can be tuned to reflect the range of forces experienced by the real raspberries. For each magnet separation setting, five measurements were taken where the mean and standard deviation are plotted.

2) *Compression force F_c variation*: To capture a “ground truth” of k_{on} and k_{off} , the compression force F_c vs distance d profile of 14 fresh raspberries were obtained for both on and off the receptacle using the measurement setup. The range of typical force displacement curves are shown in Fig. 9 indicated by the gray area. From this we can inspect a large difference between k_{on} and k_{off} of a factor of $\times 2 \sim 5$. This large difference in stiffness is one of the most challenging characteristic to reflect on the physical twin.

The coloured curves belong to different designs variants of the sensorized raspberries. For both design types A and B, the wall thickness was varied to produce thin and thick variations, resulting in a total of four designs that were tested.

When on the receptacle, we see that all designs fall within the region of a typical real raspberry (the coloured lines are in the gray area). However, the F_c variation changes greatly when off the receptacle. When the sensorized raspberry is on the receptacle and compressed, the compression force is dominated by the stiffness of the silicone material. However, when the fruit is off the receptacle, the stiffness is dominated

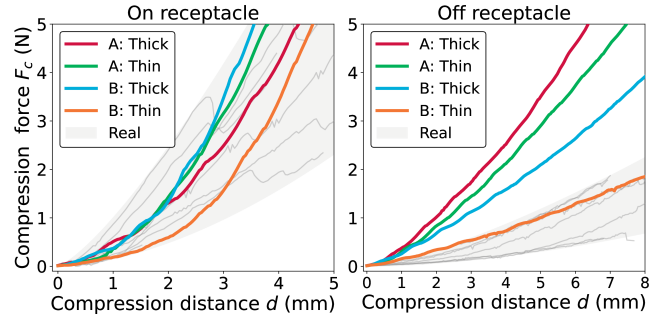


Fig. 9: Force vs compression distance plot of real and sensorized raspberries.

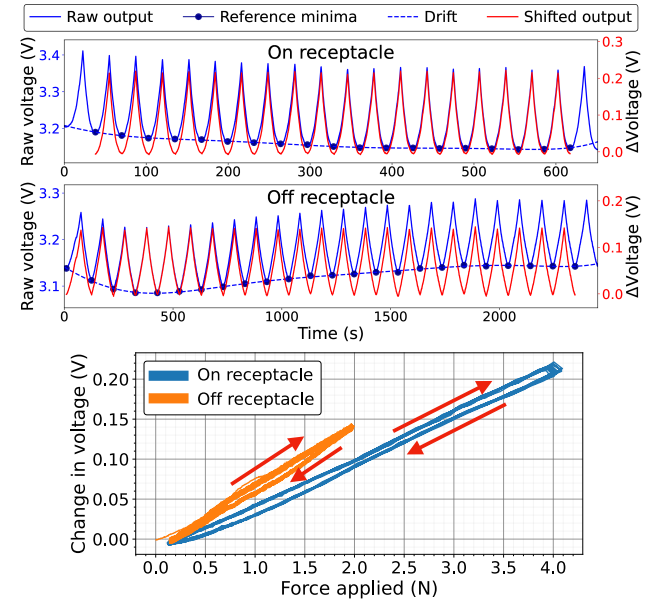


Fig. 10: Top: time series data for characterizing the fluidic sensor response. Bottom: fluidic sensor characterization.

by the geometry (provided the material is flexible), which can be seen on the right hand plot. Firstly, we see type A is stiffer than type B. Since type A has a 2 silicone layer structure, the overall thickness of the fruit is larger compared to type B. Secondly, for each type, the thinner variant had a lower stiffness. From these observations we confirm that the silicone thickness is the primary factor for k_{off} , and therefore, by varying the thickness parameter in the fabrication process, we are able to develop sensorized raspberries of a wide range of stiffness values. Finally, from the four designs the thin variant of raspberry type B closes the reality gap the best, since both the force-distance curves fall within the region of a typical real raspberry.

B. Sensor Characterization

The sensorized raspberry can be used to measure the two forces F_p and F_c applied to it. The measurement of F_p is straightforward since the raspberry is connected directly to a calibrated load cell through a string. Whereas, the measurement of F_c is done indirectly by measuring the pressure change caused by physical deformation through a tube embedded in the silicone. To demonstrate the characteristics of the fluidic sensor, strain cycles were applied to the sensorized raspberry on and off the receptacle.

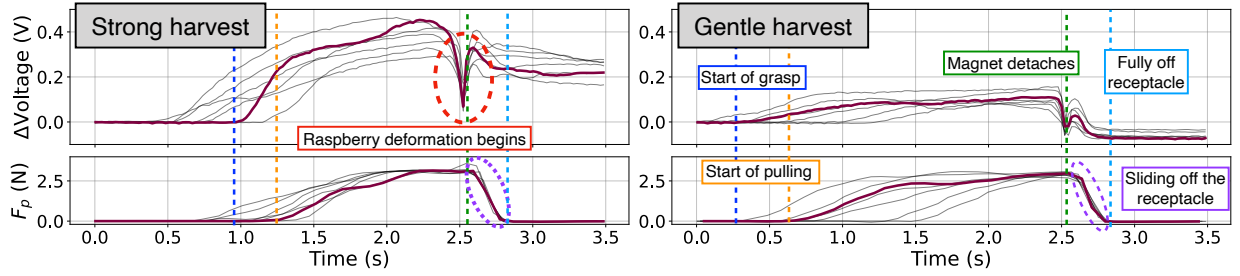


Fig. 11: Typical time series of a human harvesting the sensorized raspberry.

The curves with the solid blue line on Fig. 10 are raw voltage measurements of the sensorized raspberry. By inspection, we see that the sensitivity (i.e.: variation for each cycle) is consistent across time, but there is a drift (shown by the blue dotted line) which shifts the measurements. We hypothesize that this drift is linked to hysteresis of the silicone or tube. The drift was estimated by fitting a 8th order polynomial through least squares regression of each local minima on the raw data (marked by the blue dots).

Here we observe that the drift changes over a long time scale (in the order of 100s to 1000s). However, for this particular application we are interested in the short time scale, as the time to harvest a raspberry takes a few seconds at most. Therefore we make the assumption that over a short time scale which we are interested, the effect of the drift is negligible and we only care about the change in output. Based on this assumption, to characterize the sensitivity, the raw data is shifted by subtracting the drift curve. The drift-compensated sensor reading is given by the red solid line.

Fig. 10 plots the drift-compensated (shifted) sensor data against the ground truth force applied to it, measured by the load cell (over 20 cycles were performed). Arrows indicate the direction of hysteresis. We see for both strain cycles the response is approximately linear with little hysteresis. This is a desired response from such a sensor, and verifies the voltage output is indeed meaningful and can be used to convert voltage readings to compression force. We also observe that the force sensitivity (the gradient of the plot) changes on and off the receptacle. During each cycle the physical twin compressed 3.5mm and 9mm respectively for on and off the receptacle.

C. Harvesting Demonstration

In this section we demonstrate a simplified scenario of how the physical twin can be used to evaluate the controller of robot harvesting system, by comparing with a human.

1) *Human harvesting*: In the first experiment, a human will harvest the raspberry while the readings from the fluidic sensor and the load cell is logged (to measure F_c and F_p respectively). The aim of this experiment is to see if key events can be monitored through the time series, such as the removal of the raspberry. This way, the sensor data can be used to evaluate the quality of the harvesting motion.

Fig. 11 shows the time series for F_c and F_p measurements (top and bottom plots). All plots contain 7 time series, but one is highlighted to show a typical sample. For the left plots, a human is purposely “strongly” picking the raspberry. On

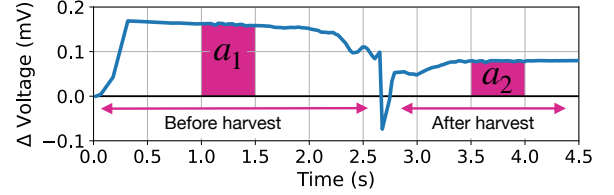


Fig. 12: Sample fluidic sensor reading during a robot harvest.

the right, the human is picking the raspberry “gently”. This strength F_c is clear from the amplitude of the fluidic sensor reading (shown by Δ Voltage).

From this time series, we can identify key events as shown on the plot. The most notable feature is the big “dip” in fluidic sensor reading which occurs consistently before the raspberry starts to detach. This is most likely caused by the tube deforming before the magnet detaches from the receptacle. This unexpected but useful feature can be used to identify the moment of detachment.

2) *Robot harvesting*: Fig. 12 shows a typical time series of the fluidic sensor response when the physical twin is harvested by the robot. Before the grasp, the fluidic sensor reading is zeroed to measure the voltage change. The magnet separation distance was set to 2mm. A simple metric to assess the picking quality is to penalize the average force applied on the raspberry both before and after the pick. From Fig. 12, we see that the force profile is steady between 1 ~ 1.5s and 3.5 ~ 4s. Therefore, the integral of the recorded data can be used to determine the average force for these regions: a_1, a_2 . *Provided the fruit is picked from the plant*, the cost metric is defined to be this average force relative to a human by subtracting the average forces for a human grasp $a_{1,h}, a_{2,h}$, as such:

$$C_1 = a_1 - a_{1,h} \quad C_2 = a_2 - a_{2,h} \quad (1)$$

In summary, C_1, C_2 represents the average force on the raspberry relative to a human *before* and *after* harvesting.

To find the optimal current set-point on the servo motor (i.e.: finding the optimal Π), the cost metric was evaluated for a range of current set-points. For each current set-point, 10 picking experiments were conducted. The average C_1, C_2 and its standard deviations are plotted in Fig. 13.

From this plot, two key observations can be made. Firstly, we see that the optimal control policy is to use the lowest current set-point (95mA) since it is minimising both metrics and can also be considered to be the most repeatable based on having the lowest standard deviation. This conclusion could have been predicted prior to the experiment, but it demonstrates a) the simple cost metric is useful and b) the

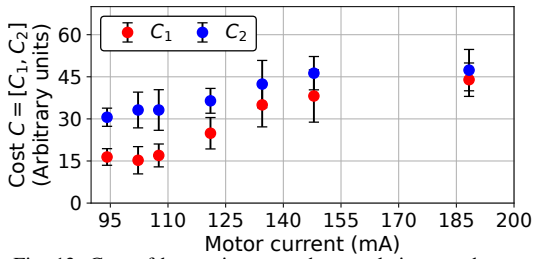


Fig. 13: Cost of harvesting a raspberry relative to a human.

sensor output/robotic setup is reliable to produce consistent measurements. The second observation is that a simple force controller is insufficient for a good picking action. For both metrics, there is a gap between the robot and human. Furthermore, we see that C_2 does not decrease as much as C_1 when the current set-point is lowered. Qualitatively, this corresponds to the raspberry always being *squished* after picking. In comparison the human holds the raspberry loosely once off the receptacle, and tunes the force applied throughout the harvesting cycle in response to tactile information. This results shows a need for sensorized grippers and a more complex controller to vary the control policy on and off the receptacle.

V. CONCLUSIONS & DISCUSSION

In this paper we presented a sensorized physical twin of a raspberry which can be used to aid in the research and development for automated robotic harvesting. By considering the pulling force F_p , compression force F_c , and the difference between the stiffness on and off the receptacle k_{on} and k_{off} , the reality gap was closed for the physical twin to match key physical properties of a real raspberry. The “fruit” of the physical twin was sensorized which produces a linear voltage output to the force applied with low drift in a short time scale. Finally, we demonstrate how the physical twin can be used with a robotic gripper setup to evaluate the quality of the picking action.

In the future, the design, fabrication, and sensor placement should be explored to improve: the effect of drift on the sensor response; the difficulty in fabrication of a type B raspberry; and better characterize how the design parameters (e.g.: wall thickness) relates to k_{on} and k_{off} . The effect of other physical properties such as the textures of the dimples could be considered for future work. Furthermore, the sensorized raspberry should be used with a more complex gripper and robotic setup to optimize a control policy (and possibly also optimize the hardware) for picking real raspberries. The visual appearance can also be improved to allow for this picking task to include computer vision within its pipeline. The stiffness of the stem/plant itself can also be incorporated into the setup by characterizing the plant properties by a spring-damper system and creating its physical twin.

REFERENCES

- [1] T. Duckett, S. Pearson, S. Blackmore, *et al.*, “Agricultural robotics: The future of robotic agriculture,” *arXiv preprint arXiv:1806.06762*, 2018.
- [2] P. L. Martin, *Farm Labor Shortages: How Real? What Response?* Center for Immigration Studies Washington DC, 2007.
- [3] R. Bogue, “Fruit picking robots: Has their time come?” *Industrial Robot: the international journal of robotics research and application*, 2020.
- [4] A. L. Gunderman, J. Collins, A. Myer, R. Threlfall, and Y. Chen, “Tendon-driven soft robotic gripper for berry harvesting,” *arXiv preprint*, 2021.
- [5] V. Ozhereliev, “Synthesis of raspberry harvesting machine actuator mechanism,” in *2015 International Conference on Mechanical Engineering, Automation and Control Systems (MEACS)*, IEEE, 2015, pp. 1–5.
- [6] E. Navas, R. Fernández, D. Sepúlveda, M. Armada, and P. Gonzalez-de-Santos, “Soft grippers for automatic crop harvesting: A review,” *Sensors*, vol. 21, no. 8, p. 2689, 2021.
- [7] Y. Sarig, “Robotics of fruit harvesting: A state-of-the-art review,” *Journal of agricultural engineering research*, vol. 54, no. 4, pp. 265–280, 1993.
- [8] G. Kootstra, X. Wang, P. M. Blok, J. Hemming, and E. Van Henten, “Selective harvesting robotics: Current research, trends, and future directions,” *Current Robotics Reports*, pp. 1–10, 2021.
- [9] S. Haag and R. Anderl, “Digital twin–proof of concept,” *Manufacturing Letters*, vol. 15, 2018.
- [10] L. Scimeca, J. Hughes, P. Maiolino, L. He, T. Nanayakkara, and F. Iida, “Action augmentation of tactile perception for soft-body palpation,” *Soft Robotics*, 2021.
- [11] J. Hughes, P. Maiolino, T. Nanayakkara, and F. Iida, “Sensorized phantom for characterizing large area deformation of soft bodies for medical applications,” in *2020 3rd IEEE International Conference on Soft Robotics (RoboSoft)*, IEEE, 2020, pp. 278–284.
- [12] M. J. Luk, D. Lobb, and J. A. Smith, “A dynamic compliance cervix phantom robot for latent labor simulation,” *Soft robotics*, vol. 5, no. 3, 2018.
- [13] *Bovine milking udder simulator*, Jan. 2020. [Online]. Available: <https://www.realityworks.com/product/bovine-milking-udder-simulator/>.
- [14] Smooth-On, *Dragon skin™ 10 fast*. [Online]. Available: <https://www.smooth-on.com/products/dragon-skin-10-fast/>.
- [15] J. Hughes, A. Spielberg, M. Chounlakone, G. Chang, W. Matusik, and D. Rus, “A simple, inexpensive, wearable glove with hybrid resistive-pressure sensors for computational sensing, proprioception, and task identification,” *Advanced Intelligent Systems*, vol. 2, no. 6, p. 2000002, 2020.
- [16] J. Hughes, S. Li, and D. Rus, “Sensorization of a continuum body gripper for high force and delicate object grasping,” in *2020 IEEE International Conference on Robotics and Automation (ICRA)*, IEEE, 2020, pp. 6913–6919.